Published in Applied Optics 27, issue 22, 4739-4746, 1988
which should be used for any reference to this work

Holographic optical scanning elements with minimum aberrations

Hans Peter Herzig and Rene Dandliker

An analytical method to design holographic optical elements for focusing laser scanners, especially disk scanners, with minimum aberrations and optimum scan line definition is reported. The results reveal that the focused spot constraint to a straight line is always astigmatic. However, by accepting small deviations from the straight line, the astigmatism can be eliminated. The second-order analytical solutions are examined with the help of geometrical ray tracing and compared with experimental results. By extending the method to higher-order approximations, it was found that the correction of the aberrations is essentially limited to the direction perpendicular to the scan line.

I. Introduction

Holographic optical elements (HOEs) can serve as the deflecting as well as the focusing element in laser scanners. They have been incorporated into supermarket point-of-sale systems,[1,2] laser beam printers,[3] and are expected to be useful in a wide range of future applications.[4,5]

No matter how the hologram is produced, it is possible to represent the hologram structure by a phase function $\Phi(x,y)$. To find the ideal phase function Φ for a special scan configuration is, in general, a complex problem. Possible solutions involve numerical optimum design methods, similar to the ones commonly used for optimizing lens systems in classical optics. A merit function has to be defined, which describes the scan quality, and by changing the wavefront parameters this merit function is minimized.[6,7] Such methods work well to find a local minimum for the specified configuration but do not yield information about a general solution nor about the influence of the different parameters. An alternative method to determine the hologram phase function Φ analytically, first introduced in 1983 by Winick and Fienup, is based on minimizing the mean-squared wavefront.[8,9] This method, however, was never applied to designing holographic scanners.

The authors are with University of Neuchatel, Institute of Microtechnology, 2000 Neuchatel, Switzerland.

Another analytical method, which is differential rather than integral, was recently presented by the authors.[10,11] There, the phase functions of holographic scanners are found by using second-order approximation for the incident and outgoing beams (astigmatic pencil of rays). The extension of the second-order theory to higher order leads to overly cumbersome formulas. This can be avoided if the aberrations, astigmatism, coma, and so on are described by a general error function rather than explicitly. This technique is discussed in the following in order to investigate the degree of freedom for the higher-order corrections.

In the experimental part, disk scanners with a wavelength shift between recording (514 nm) and reconstruction (633 nm) are described. The measured scan quality (line straightness and spot quality) is compared with the theoretical results.

II. Principle of the Error Function

A general scan geometry is assumed as sketched in Fig. 1, where a laser beam is deflected and focused by a holographic optical element (HOE). The hologram structure can be described by a phase function $\Phi(x,y)$. While displacing the HOE, the incident beam moves along a line $\mathbf{x}(s)$ in the hologram plane and the image point describes another line $\mathbf{y}(t)$ in space. A local coordinate system u,v,w is introduced, so that the w axis is normal to the hologram plane. During the scan motion, the origin of the system u,v,w, is at the center of the incident laser beam and on the line $\mathbf{x}(s)$ in the hologram plane. The outgoing wave $\Phi_P(u,v,t)$ should be ideally focused on the scan line $\mathbf{y}(t)$. However, there are in general some aberrations with respect to the ideal spherical wave $\Phi_S(u,v,t)$, which can be expressed by an error function

$$F(u,v,t) = \Phi_P(u,v,t) - \Phi_S(u,v,t). \tag{1}$$

The difference between the outgoing wave $\Phi_P(u,v,t)$ and the reconstructing wave $\Phi_r(u,v)$ in the hologram plane has to be supplied by the holographic scanning element. This difference Ψ is a function of the position t of the focus on the scan line $\mathbf{y}(t)$ in space, namely,

$$\begin{aligned}\Psi(u,v,t) &= \Phi_P(u,v,t) - \Phi_r(u,v)\\ &= \Phi_S(u,v,t) + F(u,v,t) - \Phi_r(u,v),\end{aligned} \tag{2}$$

where $\Phi_r(u,v)$ is the readout beam (plane or spherical wave), $\Phi_S(u,v,t)$ is the ideally focused (spherical) outgoing wave, and $F(u,v,t)$ is the error function.

A. Local Match of the Phase Functions

Now, we describe the scanning of the hologram phase function $\Phi(x,y)$ also in the local coordinate system u,v. The phase function then becomes $\Phi(u,v,s)$ and changes with the parameter s, which describes the position of the readout beam on $\mathbf{x}(s)$ in the hologram plane. The relation between the position s on $\mathbf{x}(s)$ in the hologram and the position t of the focus on the scan line $\mathbf{y}(t)$ in space is not *a priori* known. Within the pupil of the laser beam centered at point s, the phase function $\Phi(u,v,s)$ of the hologram should be identical to the phase function $\Psi(u,v,t)$ given in Eq. (2). In general, this condition cannot be fulfilled rigorously for all points of a continuous scan. To get at least a local match of the two phase functions Φ and Ψ, they are both expanded in Taylor series about the point $\mathbf{x}(s)$, which corresponds to the origin of the u,v-coordinate system, namely,

$$\Phi(u,v,s) = \Phi[\mathbf{x}(s)] + \left.\frac{\partial\Phi}{\partial u_i}\right|_s u_i + \frac{1}{2}\left.\frac{\partial^2\Phi}{\partial u_i\partial u_j}\right|_s u_i u_j + \ldots, \tag{3}$$

$$i,j = 1,2,$$

$$\Psi(u,v,t) = \Psi(0,0,t) + \left.\frac{\partial\Psi}{\partial u_i}\right|_t u_i + \frac{1}{2}\left.\frac{\partial^2\Psi}{\partial u_i\partial u_j}\right|_t u_i u_j + \ldots. \tag{4}$$

Here and in the following, two notations are used for the components of the spatial vectors, namely, $\mathbf{u} = (u,v,w) = (u_1,u_2,u_3)$ and $\mathbf{x} = (x,y,z) = (x_1,x_2,x_3)$.

We now require that the two series are equal up to nth order, where the first-order derivatives determine the direction and the second-order derivatives the curvature of the outgoing wave. This yields the following conditions:

$$\Phi[\mathbf{x}(s)] = \Psi(0,0,t), \tag{5a}$$

$$\left.\frac{\partial\Phi}{\partial u_i}\right|_s = \left.\frac{\partial\Psi}{\partial u_i}\right|_t \equiv h_i(t), \qquad i,j = 1,2, \tag{5b}$$

$$\left.\frac{\partial^2\Phi}{\partial u_i\partial u_j}\right|_s = \left.\frac{\partial^2\Psi}{\partial u_i\partial u_j}\right|_t \equiv h_{ij}(t), \tag{5c}$$

and equivalent for the higher-order terms $h_{i\ldots j}(t)$.

B. Local Derivatives of $\Phi(x,y)$

To find the phase function $\Phi(x,y)$, the relations between the derivatives in the two coordinate systems x,y and u,v have to be established. These relations depend on the geometry of the particular scan problem and can be formally expressed with the aid of the functions $f_{i\ldots j}$, namely,

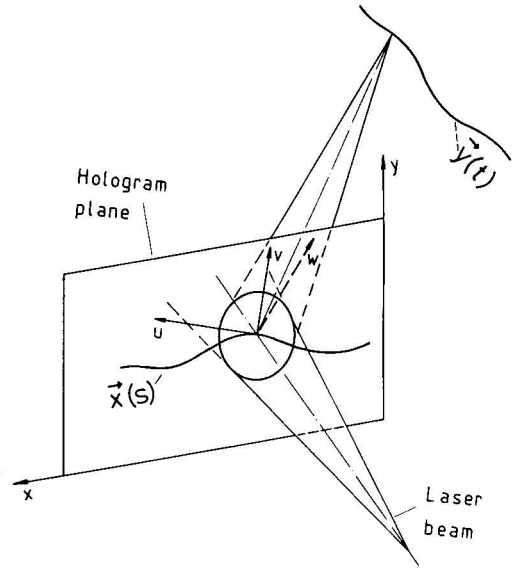

Fig. 1. General scan configuration. The hologram moves along a line $\mathbf{x}(s)$ in the hologram plane and the image point describes another line $\mathbf{y}(t)$ in space.

$$\left.\frac{\partial\Phi}{\partial x_i}\right|_s = f_i\left(\left.\frac{\partial\Phi}{\partial u_k}\right|_s\right), \tag{6a}$$

$$\left.\frac{\partial^2\Phi}{\partial x_i\partial x_j}\right|_s = f_{ij}\left(\left.\frac{\partial\Phi}{\partial u_k}\right|_s, \left.\frac{\partial^2\Phi}{\partial u_1\partial u_m}\right|_s\right). \tag{6b}$$

$$\vdots$$

Introducing Eqs. (5) into Eqs. (6) yields

$$\left.\frac{\partial\Phi}{\partial x_i}\right|_s = f_i[h_k(t)] \equiv g_i(t), \tag{7a}$$

$$\left.\frac{\partial^2\Phi}{\partial x_i\partial x_j}\right|_s = f_{ij}[h_k(t), h_{lm}(t)] \equiv g_{ij}(t). \tag{7b}$$

$$\vdots$$

The relations of Eqs. (7) have to be fulfilled simultaneously by one and the same phase function $\Phi(x,y)$ along the lone $\mathbf{x}(s)$. Thus, Eqs. (7) determine all possible solutions, for which the outgoing wave has the desired direction and the desired curvature.

For the solution of a particular scan problem, it is necessary to determine first the functions $h_{i\ldots j}(t)$. They are, following Eqs. (5), equal to the derivatives of the local phase function $\Psi(u,v,t)$ [Eq. (2)] required at the origin ($u = v = 0$) to focus the outgoing wave into the point $\mathbf{t}$ along the line $\mathbf{y}(t)$. In addition, one has to establish for the particular scan geometry the relations ($f_{i\ldots j}$) between the derivatives in the two coordinate systems x,y and u,v [Eqs. (6)] to finally get Eqs. (7) in

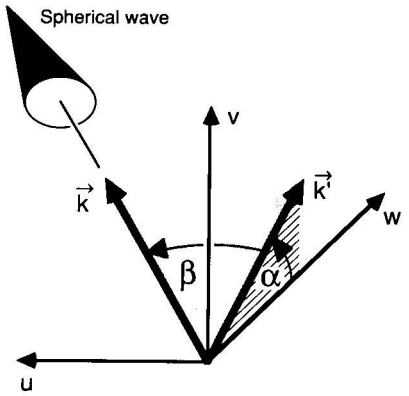

Fig. 2. Geometrical relation between the hologram plane (u,v) and the wave vector $\mathbf{k}$ of a spherical wave. $\mathbf{k}'$ is the projection of $\mathbf{k}$ onto the plane (v,w).

explicit form. The value of the phase function $\Phi(x,y)$ along $\mathbf{x}(s)$ [Eq. (5a)] follows by integration of Eq. (7a).

C. Local Derivatives of $\Psi(u,v,t)$

To calculate the derivatives of the local phase function $\Psi(u,v,t)$ at point $\mathbf{x}(s)$, it is necessary to determine first the phases of the spherical waves $\Phi_S(u,v,t)$ and $\Phi_r(u,v)$. Following Figs. 1 and 2, the spherical wave Φ_S is given by

$$\Phi_S(u,v,t) = k[(u + \sin\beta/a)^2 + (v + \sin\alpha\cos\beta/a)^2 + (\cos\alpha\cos\beta/a)^2]^{1/2}. \quad (8)$$

Since Φ_S is assumed to be ideally focused onto the scan line $\mathbf{y}(t)$, the directions $\alpha(t)$ and $\beta(t)$ and the curvature $a(t)$ are completely determined by the scan geometry. Note that $a(t)$ is negative for a convergent wave. Similarly, the readout beam is given by

$$\Phi_r(u,v,t) = k[(u)^2 + (v + \rho\sin\gamma)^2 + (\rho\cos\gamma)^2]^{1/2}, \quad (9)$$

where γ is the inclination with respect to the hologram normal and ρ is the radius of curvature.

Now, we get from Eq. (2) for the functions $h_{i\ldots j}(t) \equiv \partial^n\Psi(u,v,t)/\partial u_i \ldots \partial u_j$:

$$h_1 = \sin\beta + F_1, \quad (10a)$$

$$h_2 = \sin\alpha\cos\beta - \sin\gamma + F_2, \quad (10b)$$

$$h_{11} = a\cos^2\beta - 1/\rho + F_{11}, \quad (10c)$$

$$h_{12} = -a\sin\alpha\sin\beta\cos\beta + F_{12}, \quad (10d)$$

$$h_{22} = a(1 - \sin^2\alpha\cos^2\beta) - \cos^2\gamma/\rho + F_{22}, \quad (10e)$$

$$h_{111} = -3a^2\sin\beta\cos^2\beta + F_{111}, \quad (10f)$$

$$h_{112} = a^2\sin\alpha\cos\beta(3\sin^2\beta - 1) + \sin\gamma/\rho^2 + F_{112}, \quad (10g)$$

$$h_{122} = a^2\sin\beta(3\sin^2\alpha\cos^2\beta - 1) + F_{122}, \quad (10h)$$

$$h_{222} = 3a^2\sin\alpha\cos\beta(\sin^2\alpha\cos^2\beta - 1) + 3\sin\gamma\cos^2\gamma/\rho^2 + F_{222}, \quad (10i)$$

$$h_{1111} = 3a^3(-1 + 6\sin^2\beta - 5\sin^4\beta) + 3/\rho^3 + F_{1111}, \quad (10k)$$

$$h_{1112} = 3a^3(\sin\alpha\sin\beta\cos\beta(3 - 5\sin^2\beta) + F_{1112}, \quad (10l)$$

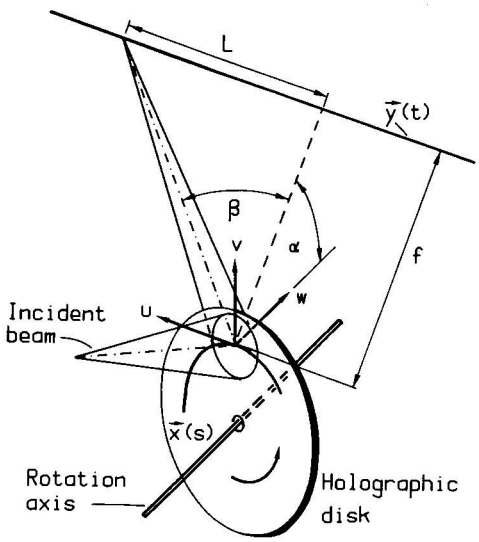

Fig. 3. Circular motion $\mathbf{x}(s)$ of the hologram (rotating disk) to generate a straight line $\mathbf{y}(t)$ in space.

$$h_{1122} = a^3(-1 + 3\sin^2\alpha\cos^2\beta + 3\sin^2\beta - 15\sin^2\alpha\sin^2\beta\cos^2\beta) + (1 - 3\sin^2\gamma)/\rho^3 + F_{1122}, \quad (10m)$$

$$h_{1222} = 3a^3\sin\alpha\sin\beta\cos\beta(3 - 5\sin^2\alpha\cos^2\beta) + F_{1222}, \quad (10n)$$

$$h_{2222} = 3a^3(-1 + 6\sin^2\alpha\cos^2\beta - 5\sin^4\alpha\cos^4\beta) + 3(1 - 6\sin^2\gamma + 5\sin^4\gamma)/\rho^3 + F_{2222}, \quad (10o)$$

where $F_{i\ldots j}(t) \equiv \partial^n F(u,v,t)/\partial u_i \ldots \partial u_j$.

Next, the local derivatives of $\Phi(u,v,s)$ have to be calculated and matched with the above $h_{i\ldots j}$. For this purpose, we consider a particular geometry, namely, a disk configuration scanner generating a straight line in space.

III. Higher-Order Analysis for Disk Configuration Scanners

The principle of the error function is now applied to a disk configuration scanner. The geometrical arrangement is shown in Fig. 3, where the polar coordinates r,ϕ are the hologram coordinates. The line $\mathbf{x}(s)$ is a circle of radius R, i.e., $\phi(s) = \phi$, $r(s) = R$. We assume for the phase function $\Phi(r,\phi)$ a fourth-order approximation perpendicular to the scan line, namely,

$$\Phi(r,\phi) = k[a_0 + a_1(r - R) + \frac{1}{2}a_2(r - R)^2 + \frac{1}{6}a_3(r - R)^3 + \frac{1}{24}a_4(r - R)^4], \quad (11)$$

where $a_k = a_k(\phi)$.

The incident beam is a spherical wave with a radius of curvature ρ and inclined at an angle γ. As shown in Fig. 3, the generated line $\mathbf{y}(t)$ should be a straight line in space. Therefore, the deflection angle $\beta(t)$ is chosen to be equal to the scan parameter $t(\beta = t)$, the inclination $\alpha(\beta)$ is constant $(\alpha = \alpha_c)$, and the curvature $a(\beta)$ is determined by the focusing condition $a(\beta) = -\cos\beta/f$.

A. Local Phase Match of the Phase Functions

To determine the functions $a_k(\phi)$, first the relations of the hologram coordinates r,ϕ and the local coordinates have to be established [Eqs. (6)]. Then the derivatives of the hologram phase function $\Phi(r,\phi)$ [Eq. (11)] and the derivatives of the functions $\Psi(u,v,t)$, i.e., $h_{i\ldots j}(t)$ in Eqs. (10), have to be matched along $\mathbf{x}(s)$ [Eqs. (7)]. This finally yields, arranged by increasing order of the derivatives of the error function,

$$F_1 = a_0'/R - \sin\beta, \tag{12a}$$

$$F_2 = a_1 - \sin\alpha\cos\beta + \sin\gamma, \tag{12b}$$

$$F_{11} = a_0''/R^2 - (a\cos^2\beta - 1/\rho) + (\sin\alpha\cos\beta - \sin\gamma)/R + F_2/R, \tag{12c}$$

$$F_{12} = a_1'/R + a\sin\alpha\sin\beta\cos\beta - \sin\beta/R - F_1/R, \tag{12d}$$

$$F_{22} = a_2 - a(1 - \sin^2\alpha\cos^2\beta) + \cos^2\gamma/\rho, \tag{12e}$$

$$F_{111} = a_0'''/R^3 + 3a^2\sin\beta\cos^2\beta - 3a\sin\alpha\sin\beta\cos\beta/R + \sin\beta/R^2 + 3F_{12}/R + F_1/R^2, \tag{12f}$$

$$F_{112} = a_1''/R^2 - 2(a\cos^2\beta - 1/\rho)/R + [a(1 - \sin^2\alpha\cos^2\beta) - \cos^2\gamma/\rho]/R + (\sin\alpha\cos\beta - \sin\gamma)/R - [a^2\sin\alpha\cos\beta(3\sin^2\beta - 1) + \sin\gamma/\rho^2] + (F_{22} - 2F_{11})/R + F_2/R^2, \tag{12g}$$

$$F_{122} = a_2'/R + 2a\sin\alpha\sin\beta\cos\beta/R - a^2\sin\beta(3\sin^2\alpha\cos^2\beta - 1) - 2F_{12}/R, \tag{12h}$$

$$F_{222} = a_3 - 3a^2\sin\alpha\cos\beta(\sin^2\alpha\cos^2\beta - 1) - 3\sin\gamma\cos^2\gamma/\rho^2, \tag{12i}$$

$$F_{1111} = a_0''''/R^4 + \ldots, \tag{12k}$$

$$\vdots$$

$$F_{2222} = a_4 + 3a^3(1 - 6\sin^2\alpha\cos^2\beta + 5\sin^4\alpha\cos^4\beta) - 3(1 - 6\sin^2\gamma + 5\sin^4\gamma/\rho^3), \tag{12o}$$

where $a_k = a_k(\phi)$ and $a_k'(\phi) = da_k/d\phi$, etc. The parameters $\alpha(\beta)$ and $a(\beta)$ of the outgoing spherical wave are given by the scan geometry [$\alpha = \alpha_c, a(\beta) = -\cos\beta/f$]. The relation $\beta(\phi)$ between the readout position ϕ and the deflection angle β is still unknown, but it will be determined later by the requirements of the scan. The errors become finally also functions of the position ϕ, namely, $F_{i\ldots j} = F_{i\ldots j}[\beta(\phi)]$.

B. Minimizing the Error Function

Now, step by step, we try to determine the coefficients $a_k(\phi)$ from Eqs. (12), while setting the errors $F_{i\ldots j}$ to zero whenever possible. To obtain the functions $a_0'(\phi)$ and $a_1(\phi)$, we can set $F_1 = 0$ in Eq. (12a) and $F_2 = 0$ in Eq. (12b) without any restrictions and for any $\beta(\phi)$. When setting $F_{11} = 0$, an additional equation for $a_0(\phi)$ is obtained from Eq. (12c), which contains $a_0''(\phi)$. Since the relation $d(a_0')/d\phi = a_0''$ has to be fulfilled, we now obtain the scan equation

$$d\beta/d\phi - Ra(\beta)\cos\beta + R/(\rho\cos\beta) + \sin\alpha - \sin\gamma/\cos\beta = 0, \tag{13}$$

which determines the function $\beta(\phi)$.[10] At this point we have $F_1 = F_2 = F_{11} = 0$ realized and $\beta(\phi), a_0(\phi), a_1(\phi)$ determined.

Therefore, the error F_{12} in Eq. (12d) is completely determined and cannot be set to zero, unless an additional degree of freedom is introduced. As found in a previous paper[10] for the astigmatism, it is not possible to compensate for the error F_{12} when the scanning is constrained to a straight line ($\alpha = \alpha_c$). Only by accepting a curved scan line $\alpha(\phi)$ is it possible to set $F_{12} = 0$.[11] Equation (12d) then determines the required deviation $\Delta\alpha(\phi) = \alpha(\phi) - \alpha_c$. It follows [see Ref. 12, Eqs. (3.29) and (3.30), p. 38] that

$$d\alpha/d\phi = -\tan\beta[(\tan\alpha/\cos\beta)(R/\rho - \sin\gamma) - \cos\alpha]. \tag{14}$$

The structure of the remaining Eqs. (12e)–(12o) shows that only the errors F_{22}, F_{222}, and F_{2222} can be set to zero by choosing the functions $a_2(\phi)$, $a_3(\phi)$, and $a_4(\phi)$ appropriately, whereas all other $F_{i\ldots j}$ are entirely given by the previously determined $a_k(\phi)$ and their derivatives. Note that $F_{22} = 0$ determines an optimum solution for $a_2(\phi)$, but it does not necessarily correspond to an optimized astigmatism,[10] except for $F_{12} = 0$.

C. Discussion of Higher-Order Corrections

The analytical method reported in the preceding sections requires that for all scan positions the outgoing beam is focused on the generated scan line $\mathbf{y}(t)$ with a minimum of astigmatism. If the geometry of the scan configuration and the scan line $\mathbf{y}(t)$ is specified, the solution is already determined up to second order and with it most of the higher-order aberrations, which cannot be compensated by higher-order terms in $\Phi(x,y)$. In particular, the coefficient a_0 determines the phase function on the line $\mathbf{x}(s)\{\Phi[\mathbf{x}(s)] = ka_0\}$ and the scan equation [Eq. (13)] describing the relation $\beta(\phi)$. Higher-order corrections are essentially limited to the direction perpendicular to the scan line $\mathbf{x}(s)$. But they cannot compensate for the errors on the scan line that remain from the second-order theory.

Setting the errors $F_{i\ldots j}$ to zero whenever possible is a straightforward analytical method. Such a procedure would yield phase functions $\Phi(x,y)$ for which the holographic scanners have low aberrations and distortions. However, the optimum solution may correspond to a more balanced distribution of the errors $F_{i\ldots j}$. This can be done, for example, by using numerical methods which are beyond the scope of this paper.

IV. Experimental Investigations

This section reports the experimental investigations of our calculated holographic disk scanners, which were recorded with the aid of computer-generated holograms (CGHs). First the setups for recording and reconstruction are described. Then the experimental results for three different disk scanners are presented.

A. Realization of the Holographic Scanners

For given readout geometry and wavelength λ_r, the holographic scanner phase function $\Phi(x,y)$ can be cal-

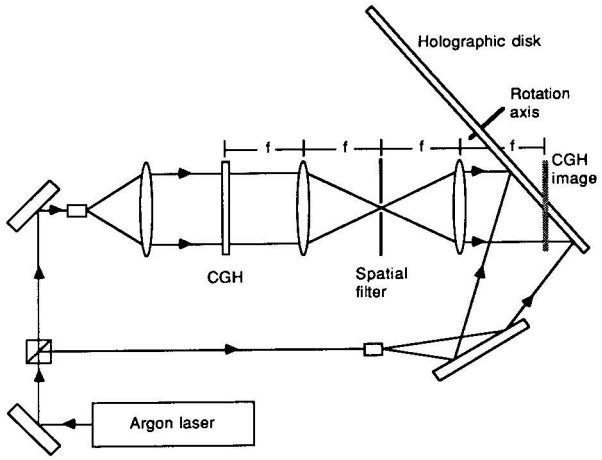

Fig. 4. Recording setup to realize a holographic scanning element with the aid of a computer-generated hologram (CGH).

culated according to Eq. (11). Phase Φ is formed by recording the interference of a spherical object wave Φ_O and an aspherical reference wave Φ_R at the recording wavelength $\lambda_R(\neq\lambda_r)$. The relation between the phases in the hologram plane is then given by

$$\Phi = \Phi_O - \Phi_R. \tag{15}$$

The spherical wave Φ_O is chosen so that the Bragg condition is fulfilled and the spatial bandwidth of the aspherical wave Φ_R is low.[12] The aspherical wave is generated with the aid of a CGH.

The experimental setup for recording is shown in Fig. 4. The laser beam is split into a plane wave branch for the reference wave and a spherical branch for the object wave. The CGH is inserted into the plane wave branch of the recording setup. A telescopic lens system creates a 1:1 image of the CGH at the holographic scanner, which is inclined with respect to the CGH image plane. The phase function Φ_{CGH} necessary to generate Φ_R in the hologram plane can be calculated with the aid of the ray tracing method, taking into account the optical path length between the CGH image plane and the hologram plane. The carrier frequency ν of the CGH, which is a binary hologram, separates the higher-order wavefronts from the zero order, so that by using a spatial filter only the first order is allowed to pass, thereby forming the desired aspherical wave.

The CGH also includes a correction for the change in wavelength between recording and readout of the scanning element.[12] The wavelength shift is imposed because the spectral sensitivity of the high efficiency photosensitive materials is typically <520 nm, whereas the wavelength of the readout sources, used for the laser scanners, are >630 nm (e.g., He–Ne, AlGaAs).

B. Experimental Setup for Measuring the Performance of the Scanners

In the following we shall describe the experimental setup for measuring the image spot quality and its position with respect to a straight scan line.

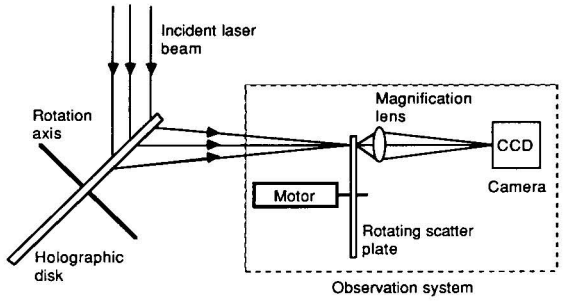

Fig. 5. Experimental setup for measuring the performances of the holographic scanners. The holographic disk rotates around its axis and generates a line perpendicular to the drawing plane. The observation system is translated along the generated line to determine the image point for different scan positions.

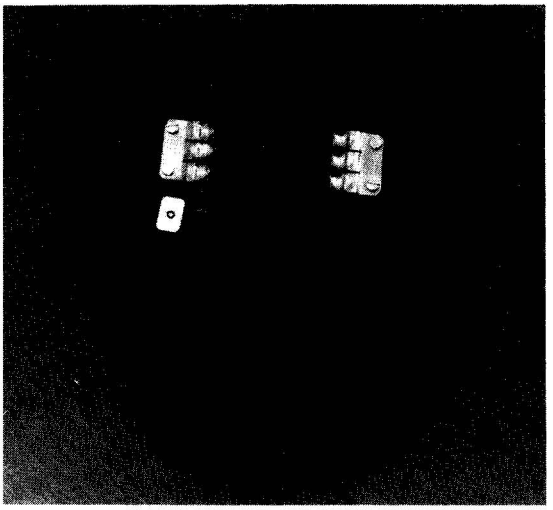

Fig. 6. Holographic optical element corresponding to one segment of a disk scanner.

We determined the spot quality of the holographic scanning elements at different scan positions. Figure 5 shows the experimental setup for measuring the image spot quality and its position with respect to a straight line. An incident laser beam is deflected by the holographic disk scanner and focused on a scatter plate at the image plane. The holographic disk rotates around its axis and generates a scan line $\mathbf{y}(t)$ in the image plane; the scan line is perpendicular to the drawing plane. The observation system magnifies the image point and detects the spot quality with a CCD camera. To avoid the disturbing laser speckles, the scattering plate was rotated. During scanning, the observation system, including the scatter plate, was translated parallel to the generated scan line. The scan line deviation Δy of the spot as a function of the scan length L was measured with the aid of a micrometer mounted on the observation system.

In our experiments, the scanning elements were segments of a disk, as shown in Fig. 6. A complete holographic scanner would, of course, be a disk with several holograms, each generating its own line.

V. Conclusions

An analytical method for the design of holographic optical elements (HOE) for focusing laser scanners with minimum aberrations and optimum scan line definition is reported. We were especially interested in disk scanners that generate straight lines in space. We found that a circular motion cannot generate a straight line without astigmatism in the focal spot. By accepting a slightly curved scan line, the astigmatism can be eliminated and the spot quality improved.

The second-order analytical solutions were examined with the help of geometrical ray tracing and compared with experimental results. We measured spot diameters (at half-intensity) of $<60\ \mu m$ for a maximum scan line deviation of $\pm 30\ \mu m$ and $<85\ \mu m$ for a maximum scan line deviation of $\pm 8\ \mu m$, for any position within the scan length of ± 105 mm at an image plane distance of 300 mm. The experimental results and the theoretical predictions are in a good agreement.

Extending the method to higher-order approximations, we found that aberrations perpendicular to the scan line can be minimized with appropriate corrections of the hologram phase function. However, astigmatism and other higher-order aberrations, especially in the scan direction, cannot be removed completely. It is possible that numerical optimum design methods could be used to further improve the solutions found by our analytical approach.

Our design method need not be restricted to holographic optical scanning elements. For example, other HOEs which have to transform a continuous set of input wavefronts into a continous set of output wavefronts can also be designed with our method.

This research was performed in close collaboration with the Optical Systems Department of the Centre suisse d'électronique et de microtechnique S.A., Neuchâtel, where the CGHs were produced. In particular, we wish to thank H. Buczek, head of this department, for his helpful advice and A. A. Friesem from the Weizmann Institute of Science, Rehovot, Israel, for many fruitful discussions.

References

1. L. D. Dickson, G. T. Sincerbox, and A. D. Wolfheimer, "Holography in the IBM 3687 Supermarket Scanner," IBM J. Res. Dev. **26,** 228 (1982).
2. H. Ikeda, M. Ando, and T. Inagaki, "Aberration Corrections for a POS Hologram Scanner," Appl. Opt. **18,** 2166 (1979).
3. H. Funato, "Holographic Scanner for Laser Printer," Proc. Soc. Photo.-Opt. Instrum. Eng. **390,** 174 (1983).
4. L. Beiser, "Imaging with Laser Scanners," Opt. News (Nov. 1986), pp. 10–16.
5. Y. Ono and N. Nishida, "Holographic Laser Scanners for Multidirectional Scanning," Appl. Opt. **22,** 2128 (1983).
6. H. Iwaoka and T. Shiozawa, "Aberration-Free Linear Holographic Scanner and Its Application to a Diode-Laser Printer," Appl. Opt. **25,** 123 (1986).
7. Y. Ono and N. Nishida, "Holographic Optical Elements with Optimized Phase-Transfer Functions," J. Opt. Soc. Am. A **3,** 139 (1986).
8. K. A. Winick and J. R. Fienup, "Optimum Holographic Elements Recorded with Nonspherical Wave Fronts," J. Opt. Soc. Am. **73,** 208 (1983).
9. J. Kedmi and A. A. Friesem, "Optimized Holographic Optical Elements," J. Opt. Soc. Am. A **3,** 2011 (1986).
10. H. P. Herzig and R. Dandliker, "Holographic Optical Scanning Elements: Analytical Method for Determining the Phase Function," J. Opt. Soc. Am. A **4,** 1063 (1987).
11. H. P. Herzig and R. Dandliker, "Design Rules for Holographic Optical Scanning Elements," Proc. Soc. Photo-Opt. Instrum. Eng. **812,** 86 (1987).
12. H. P. Herzig, "Holographic Optical Scanning Elements," Ph.D. Thesis U. Neuchâtel, Switzerland (1987).